

Cite this: *RSC Adv.*, 2017, 7, 36852

Enhanced hydrogen storage properties of a dual-cation (Li^+ , Mg^{2+}) borohydride and its dehydrogenation mechanism†

 Liuting Zhang,^{‡ab} Jianguang Zheng,^{‡ac} Xuezhong Xiao,^{ID*ab} Xiulin Fan,^d Xu Huang,^a Xinlin Yang^b and Lixin Chen^{ID*ac}

In this paper, we present a new method to synthesize a dual-cation (Li^+ , Mg^{2+}) borohydride. It is found that Li-Mg-B-H is formed by mechanical milling a mixture of LiBH_4 and MgCl_2 with a molar ratio of 3 : 1 in diethyl ether (Et_2O) and a subsequent heating process. The morphology and structure of the as-prepared Li-Mg-B-H compound are studied by SEM, XRD, FTIR and NMR measurements. Further experiments testify that Li-Mg-B-H can release approximately 12.3 wt% of hydrogen under 4 bar initial hydrogen pressure from room temperature to 500 °C and reach a maximum desorption rate of 13.80 wt% per h at 375 °C, which is 30 times faster than that of pristine LiBH_4 . Thermal analysis indicates that the decomposition process of the new compound involves three steps: (1) Li-Mg-B-H first decomposes into LiBH_4 and MgH_2 and synchronously releases a number of H_2 molecules; (2) MgH_2 decomposes to Mg and H_2 ; (3) LiBH_4 reacts with Mg , generating H_2 , MgB_2 and LiH . Moreover, Li-Mg-B-H is proved to be partially reversible, which can release 5.3 wt% hydrogen in the second dehydrogenation process. The strategy of altering the χ_p of metal ions in borohydrides may shed light on designing dual-cation borohydrides with better hydrogen storage performance.

Received 13th June 2017

Accepted 21st July 2017

DOI: 10.1039/c7ra06599j

rsc.li/rsc-advances

Introduction

Hydrogen, which produces nearly zero pollutant emission from power generators, is regarded as one of the most promising cost-effective and renewable energy carriers during past decades. However, a safe hydrogen storage technology with a high energy density still challenges scientists worldwide.^{1,2} LiBH_4 , which has high gravimetric and volumetric hydrogen densities (18.5 wt% and 121 $\text{kg}\cdot\text{H}_2$ per m^3), is regarded as one of the most promising hydrogen storage materials.^{3,4} Nevertheless, LiBH_4 is thermodynamically stable and kinetically sluggish in dehydrogenation. Besides, extremely rigorous temperature and pressure conditions are required for LiBH_4 to re-form, which severely limits its practical on-board automobile application.

In past decades, numerous attempts have been carried out to destabilize LiBH_4 , including catalyst doping,^{5–10} reactive composite formation,^{11–16} nanoconfinement^{17,18} and a combination of strategies.^{19–26} Recently, Orimo *et al.* found that the thermodynamic stability of ionic borohydrides can be correlated fairly well with the Pauling electronegativity χ_p of metal ions, M^{n+} ; the higher χ_p of M^{n+} , the less stable $\text{M}(\text{BH}_4)_n$ will be.^{27,28} This finding suggests that the thermodynamic stability of LiBH_4 can be tuned by using metal ions M^{n+} with higher χ_p to partially substitute the Li cations to form a dual-cation borohydride $\text{LiM}(\text{BH}_4)_{n+1}$. Employment of this strategy has yielded several novel dual-cation borohydrides. Jiang *et al.*²⁹ successfully synthesized a new Li-Ca-B-H complex borohydride with its first dehydrogenation step started at *ca.* 70 °C, much lower than those of pristine LiBH_4 and $\text{Ca}(\text{BH}_4)_2$. Choudhury *et al.*²⁶ prepared a new complex hydride $\text{LiMn}(\text{BH}_4)_3$ with a 3 : 1 ratio of precursor materials LiBH_4 and MnCl_2 via the solid-state mechano-chemical process. Thermogravimetric analysis (TGA) of $\text{LiMn}(\text{BH}_4)_3$ indicated that *ca.* 8.0 wt% hydrogen can be released between 135 °C and 155 °C in a single dehydrogenation step. Kim *et al.*³⁰ found that ball milling LiBH_4 and ScCl_3 produced LiCl and a unique crystalline hydride, which has been unequivocally identified via multinuclear solid-state nuclear magnetic resonance (NMR) to be $\text{LiSc}(\text{BH}_4)_4$. Fang *et al.*³¹ claimed that they had synthesized a dual-cation borohydride directly from LiBH_4 and $\text{Mg}(\text{BH}_4)_2$ with molar ratio of 1 : 1. Rapid hydrogen release from the $\text{LiBH}_4/\text{Mg}(\text{BH}_4)_2$ sample was

^aState Key Laboratory of Silicon Materials, School of Materials Science and Engineering, Zhejiang University, Hangzhou 310027, P.R. China. E-mail: xzxiao@zju.edu.cn; lxchen@zju.edu.cn; Fax: +86 571 87951152; Tel: +86 571 87951152

^bSchool of Energy and Power, Jiangsu University of Science and Technology, Zhenjiang 212003, P.R. China

^cKey Laboratory of Advanced Materials and Applications for Batteries of Zhejiang Province, Hangzhou 310013, P.R. China

^dDepartment of Chemical and Biomolecular Engineering, University of Maryland, College Park, MD 20742, USA

† Electronic supplementary information (ESI) available. See DOI: 10.1039/c7ra06599j

‡ Liuting Zhang and Jianguang Zheng contributed equally.



initiated at around 240 °C, which is about 30 °C and 170 °C lower than that of LiBH_4 and $\text{Mg}(\text{BH}_4)_2$. However, Bardají *et al.*³² investigated the physical mixture of $x\text{LiBH}_{4(1-x)}\text{Mg}(\text{BH}_4)_2$ with $x = 0, 0.10, 0.25, 0.33, 0.40, 0.50, 0.60, 0.66, 0.75, 0.80, 0.90, 1$ and found it was only a physical mixture but not a dual-cation borohydride. The eutectic composition was found to exist at $0.50 < x < 0.60$ exhibiting a eutectic melting at 180 °C and the decomposition of the material begins right after the melting. At 270 °C the $x = 0.50$ composite release about 7.0 wt% of hydrogen. Therefore no confirmed synthesis of dual-cation $\text{LiMg}(\text{BH}_4)_3$ has been reported yet.

Inspired by the theory and experiments above, it seems that thermodynamic stability of LiBH_4 can be decreased by introducing metal ions with higher χ_p . Besides, the most feasible way to synthesize a dual-cation borohydride is milling LiBH_4 with metal chloride. In this paper, we focus on the Li–Mg–B–H system, aiming to elucidate the possible formation of a dual-cation borohydride *via* wet-milling LiBH_4 and MgCl_2 in Et_2O . The samples are carefully characterized and determined by the SEM, XRD, FTIR and NMR measurements, and their hydrogen storage properties have been investigated.

Experimental section

All sample operations were performed in an Ar-filled glovebox, which was equipped with a circulative purification system to maintain the H_2O and O_2 levels below 0.1 ppm. LiBH_4 (assay 95%, Alfa Aesar), NaBH_4 (96%, Sinopharm Chemical Reagent co., Ltd) and MgCl_2 (assay 98%, Sigma) were used as starting materials. Et_2O (C_4H_{10} , 99.5%, Hangzhou Chemical Reagent co., Ltd) was used as solvent. 2 g mixture of LiBH_4 and MgCl_2 in a molar ratio of 3 : 1 together with 60 mL of Et_2O was put into a stainless steel vial with a ball-to-power ratio of 20 : 1. The ball milling process was carried out on a planetary ball mill (QM-3SP4, Nanjing, China) under 1 MPa high purity H_2 (99.999%) at a speed of 400 rpm. The milling process was paused 0.1 h for every 0.4 h to avoid the increase of temperature. The prepared liquid mixture flowed through a homemade filtration device to remove the by-product LiCl . Then the filtered liquid was heated to 205 °C in a homemade vial and vacuumed at the same time for 2 h to eliminate the solvent, and the dry products were obtained. In comparison, $\text{Mg}(\text{BH}_4)_2$ was synthesized from MgCl_2 and NaBH_4 in dried diethyl ether as described previously.³³

Differential scanning calorimetry (DSC) measurements were conducted on a Netzsch STA 449 F3 analyzer under high purity flowing argon conditions (99.999%, 50 mL min^{-1}). The hydrogen desorption/absorption properties were quantitatively evaluated by a volumetric method on a Sieverts-type apparatus, where the experimental data were monitored and recorded automatically. About 150 mg of sample was used for each temperature programmed desorption (TPD) measurement. In the temperature ramp experiments, the temperature was gradually elevated from room temperature to 500 °C at a heating rate of 2 °C min^{-1} for dehydrogenation (under 4 bar initial hydrogen pressure) and hydrogenation (initially hydrogen pressure being 100 bar). For isothermal examination, the sample was heated to a desired temperature rapidly and kept during the entire measurement.

Morphology and elemental distribution of samples were identified by scanning electron microscopy (SEM, Hitachi SU-70) equipped with an energy dispersive X-ray spectroscopy (EDX, HORIBAX-Max). X-ray diffraction analysis was conducted on an X'Pert Pro X-ray diffractometer (PANalytical, Netherlands) with Cu K α radiation at 40 kV and 40 mA. A special container fully filled with high purity Ar was prepared to avoid air exposure during sample transferring and testing. Fourier transform infrared (FTIR) spectra were obtained with a Bruker Tensor 27 unit in transmission mode. Solid state magic angle spinning (MAS) NMR spectra were obtained using a Bruker Avance 300 MHz spectrometer with a wide bore 7.04 T magnet and employing a boron-free Bruker 7 mm CPMAS probe. The spectral frequency was 75 MHz for the ^{11}B nucleus and the NMR shifts are reported in parts per million (ppm) externally referenced to NaBH_4 . The powder materials were packed into 7 mm ZrO_2 rotors in an argon-filled glovebox and were sealed with tight fitting Kel-F caps. The one-dimensional (1D) ^{11}B MAS NMR spectra were acquired after a 1.7 μs single $\pi/2$ pulse (corresponding to radio field strength of 92.6 kHz). The spectra were recorded at a MAS spinning rate of 5 kHz. The recovery delay was set to 5 s. Spectra were acquired at 20 °C.

Results and discussion

Morphology and structure of as-prepared samples

SEM images of as-prepared samples are presented in Fig. 1. LiBH_4 has a flocculent surface in Fig. 1a ($\times 1.00\text{k}$) and larger magnification picture (Fig. 1b) shows a smooth surface with small holes in it. Comparing Fig. 1c with 1e, the as-synthesized $\text{Mg}(\text{BH}_4)_2$ presents similar morphology with the as-prepared Li–Mg–B–H but with worse electroconductivity. Under enlarged magnification, as-prepared Li–Mg–B–H shows a smooth surface similar to that of LiBH_4 , while a much rougher surface with small particles on it emerges in the as-synthesized $\text{Mg}(\text{BH}_4)_2$. In addition, as we can see from the EDX mapping data of Li–Mg–B–H in Fig. S1,[†] the Mg and B elements are dispersed homogeneously in the Li–Mg–B–H matrix, further demonstrating the possibility of the formation of a new compound.

In order to determine the microstructures of as-prepared Li–Mg–B–H, XRD and FTIR examinations of LiBH_4 , as-synthesized $\text{Mg}(\text{BH}_4)_2$ and as-prepared Li–Mg–B–H were recorded, presented in Fig. 2. The XRD pattern of as-synthesized $\text{Mg}(\text{BH}_4)_2$ in Fig. 2c shows diffraction peaks of both low temperature phase $\alpha\text{-Mg}(\text{BH}_4)_2$ and high temperature phase $\beta\text{-Mg}(\text{BH}_4)_2$,³⁴ indicating that the as-synthesized $\text{Mg}(\text{BH}_4)_2$ was a mixture of $\alpha\text{-Mg}(\text{BH}_4)_2$ and $\beta\text{-Mg}(\text{BH}_4)_2$. The physical mixture of LiBH_4 and $\text{Mg}(\text{BH}_4)_2$ with a molar ratio of 1 : 1 (Fig. 2e) shows the total diffraction peaks of LiBH_4 and $\text{Mg}(\text{BH}_4)_2$. The appearance of LiCl in Fig. 2d and in the filter residue (Fig. S2[†]) demonstrates the reaction between LiBH_4 and MgCl_2 occurred during the wet-chemical ball milling process. Combining all the analyses of the diffraction patterns of relevant samples, peaks at $2\theta = 16^\circ, 18.1^\circ, 19.1^\circ, 25^\circ, 27.3^\circ$ in Fig. 2d should be assigned predominately to a new phase, this agrees well with Fang's³¹ conclusion and these new phases may come from a new dual-cation borohydride.



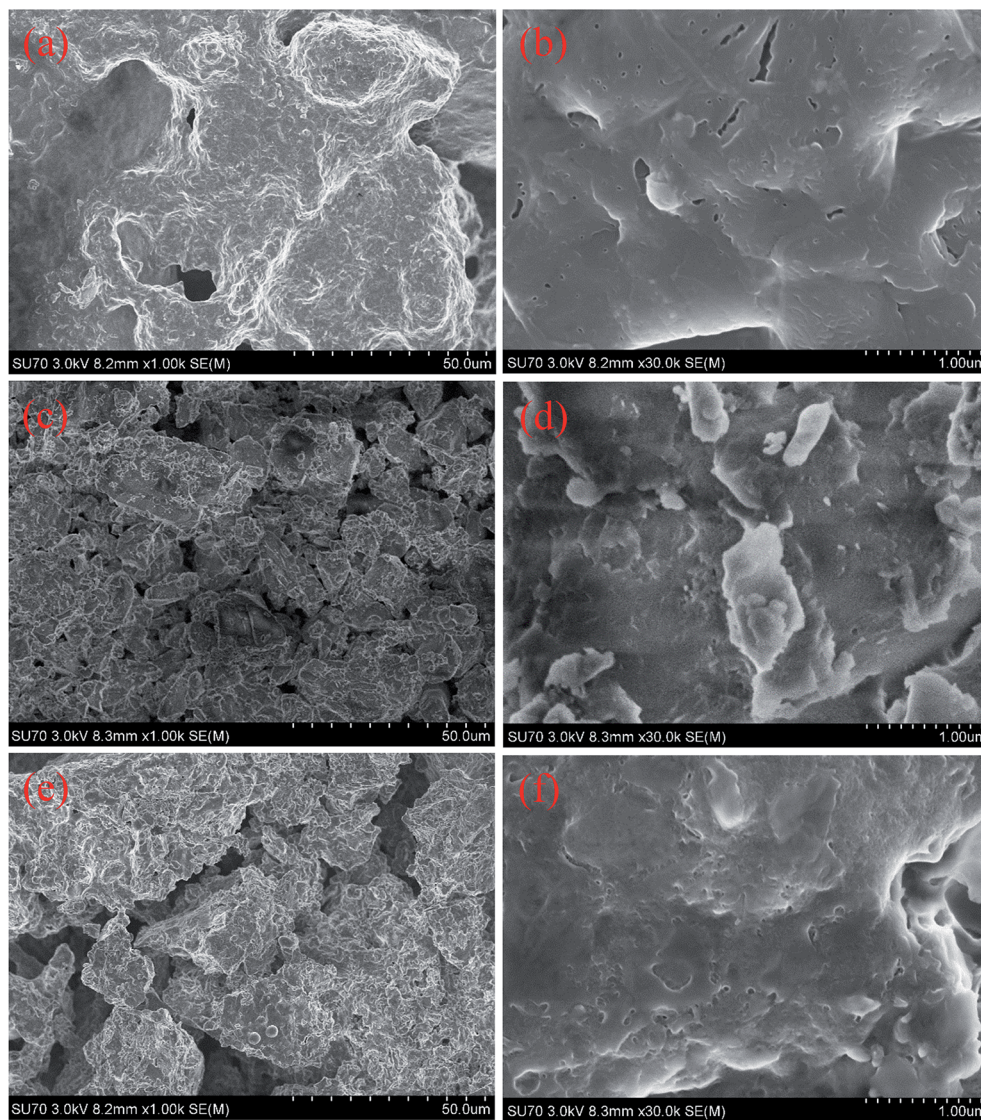


Fig. 1 SEM images of (a, b) LiBH_4 , (c, d) as-synthesized $\text{Mg}(\text{BH}_4)_2$ and (e, f) as-prepared Li-Mg-B-H .

From the results of FTIR measurements, typical features of $[\text{BH}_4]^{1-}$ group can be readily observed in the spectra, *i.e.* the stretching and deformation of B-H bonds in the regions between 2200 and 2400 cm^{-1} and 1100 and 1300 cm^{-1} , respectively.³ The B-H absorption band is split into three contributions at 2386 cm^{-1} , 2291 cm^{-1} , and 2223 cm^{-1} . The B-H bending vibration in LiBH_4 is at 1125 cm^{-1} while that of $\text{Mg}(\text{BH}_4)_2$ is split into two contributions at 1125 cm^{-1} and 1267 cm^{-1} . The presence of an absorption band around 1033 cm^{-1} contributes to $\alpha\text{-Mg}(\text{BH}_4)_2$.³⁴ Furthermore, the absorption band in the regions between 650 and 700 cm^{-1} originate from $\text{Mg}(\text{BH}_4)_2$. The mixed LiBH_4 and $\text{Mg}(\text{BH}_4)_2$ shows all the bands of LiBH_4 and $\text{Mg}(\text{BH}_4)_2$, as displayed in Fig. 2e. Combining the above analysis, we can see that as-prepared Li-Mg-B-H sample shares the same stretching and deformation of B-H bonds with physically combined $\text{LiBH}_4\text{-Mg}(\text{BH}_4)_2$ but also has slight difference. It does not show the absorption band in the regions between 650 and 700 cm^{-1} , which originate from $\text{Mg}(\text{BH}_4)_2$.

In order to further clarify the specificity of Li-Mg-B-H , NMR measurements were adopted to test the chemical shift of ^{11}B of LiBH_4 , as-synthesized $\text{Mg}(\text{BH}_4)_2$, as-prepared Li-Mg-B-H , physical mixed $\text{LiBH}_4\text{-Mg}(\text{BH}_4)_2$, respectively. If the as-prepared Li-Mg-B-H is a physical mixture, the chemical shift peak of ^{11}B should be a combination of those of LiBH_4 and $\text{Mg}(\text{BH}_4)_2$. However, as the NMR results shown in Fig. 3, as-prepared Li-Mg-B-H exhibits different peaks. The peaks of LiBH_4 , $\text{Mg}(\text{BH}_4)_2$ and physical mixed $\text{LiBH}_4\text{-Mg}(\text{BH}_4)_2$ appear at -40.30 , -39.89 , and -40.02 ppm , respectively. The peak of physical mixed sample is asymmetric (a shoulder at around -45 ppm) and the chemical shift is just between -40.30 and -39.89 ppm , which proves the nature of physical mixing. However, the chemical shift of ^{11}B in the primary new Li-Mg-B-H compound is -39.59 ppm , indicating a new chemical circumstance for B. Considering that the starting ingredient are $3\text{LiBH}_4\text{-MgCl}_2$, the new compound is more likely to be $\text{LiMg}(\text{BH}_4)_3$. Due to the limitation of laboratory equipment, currently we cannot



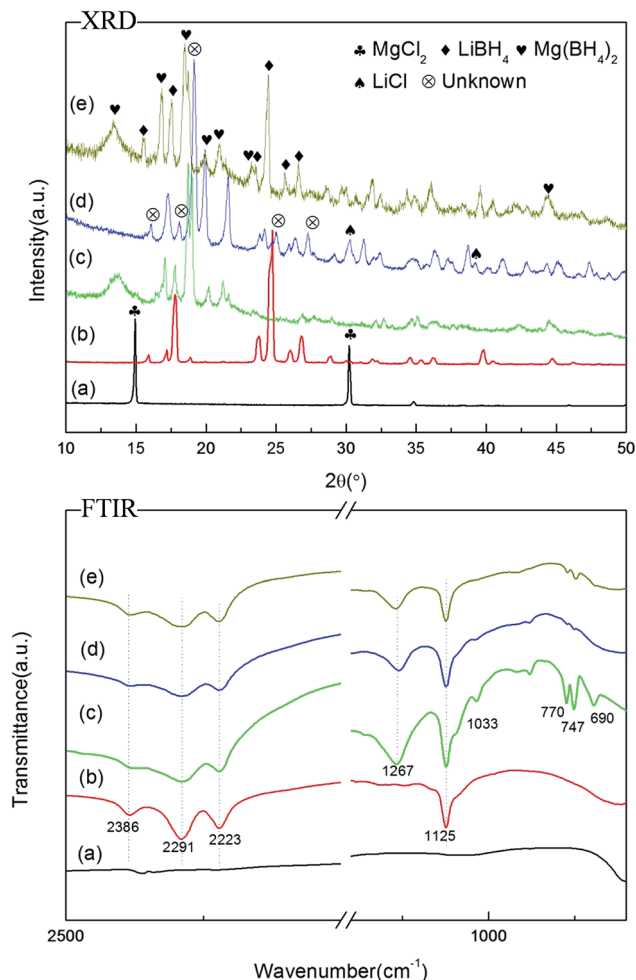


Fig. 2 XRD patterns and FTIR spectra of (a) MgCl_2 , (b) LiBH_4 , (c) as-synthesized $\text{Mg}(\text{BH}_4)_2$, (d) as-prepared Li-Mg-B-H , (e) physical mixed $\text{LiBH}_4\text{-Mg}(\text{BH}_4)_2$.

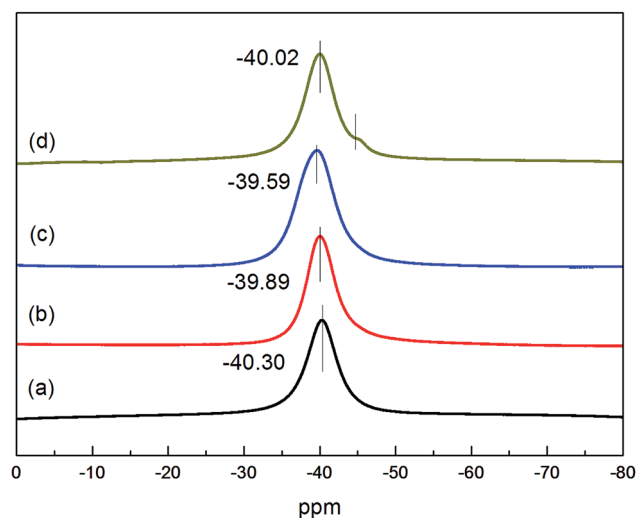


Fig. 3 ^{11}B MAS NMR spectra of the (a) LiBH_4 , (b) as-synthesized $\text{Mg}(\text{BH}_4)_2$, (c) as-prepared Li-Mg-B-H , (d) physical mixed $\text{LiBH}_4\text{-Mg}(\text{BH}_4)_2$.

measure out the exact composition of the new compound. Through the above discussion, the as-prepared Li-Mg-B-H is not just a physical mixture of LiBH_4 and $\text{Mg}(\text{BH}_4)_2$ but a new dual-cation borohydride.

Hydrogen desorption performance

The DSC-MS characteristics of as-prepared Li-Mg-B-H are shown in Fig. 4. DSC curve exhibits five endothermic peaks, which correspond to the structure transition (104.4°C), melting (174.2°C), and decomposition of as-prepared Li-Mg-B-H (260.9 , 358.3 , 391.6°C), respectively.¹² MS results demonstrate that the gas released is pure H_2 without B_2H_6 , and MS desorption peak temperatures are in good agreement with DSC results. Kou *et al.*³⁵ found that initial hydrogen pressure had a great impact on the dehydrogenation of $2\text{LiBH}_4\text{-MgH}_2$ system. Under four bar initial hydrogen pressure, LiBH_4 reacts with Mg to yield MgB_2 , which is essential for the reversibility of this system. Four bar initial hydrogen pressure was also adopted to explore its effect on the decomposition of Li-Mg-B-H . Fig. S3† presents the XRD patterns of the decomposed sample of Li-Mg-B-H at different initial hydrogen pressures. We can see from Fig. S3† that when hydrogen pressure raises to 4 bar a tip bumps up at around 42° , which is the main diffraction peak of MgB_2 . This testifies that four bar initial hydrogen pressure can help to form MgB_2 during decomposition. Hence, variable temperature hydrogen desorption behavior of the as-prepared samples was conducted using a TPD apparatus under four bar initial hydrogen pressure.

Fig. 5 shows TPD curves of LiBH_4 , as-synthesized $\text{Mg}(\text{BH}_4)_2$ and as-prepared Li-Mg-B-H . It was observed that the decomposition of the pristine LiBH_4 started sluggishly at 320°C , resulting in a final release of 4.3 wt% hydrogen at 500°C . As-synthesized $\text{Mg}(\text{BH}_4)_2$ first decomposed at 300°C , quickly releasing a large amount of H_2 with the elevating temperature and finally reached a 11.7 wt% hydrogen release at 500°C . Worth-noting, the operating temperature for hydrogen desorption of as-prepared Li-Mg-B-H was significantly reduced to 250°C , 70°C and 50°C lower compared to that of pristine LiBH_4 and as-synthesized $\text{Mg}(\text{BH}_4)_2$, respectively. In total, 12.3 wt% hydrogen was released from the dual-cation borohydride, which is three times larger comparing to that of pristine LiBH_4 (4.3 wt%) and higher than that of as-synthesized $\text{Mg}(\text{BH}_4)_2$ (11.7 wt%). Furthermore, the new compound can release hydrogen at a rate of 13.80 wt% per h at 375°C , just as fast as as-synthesized $\text{Mg}(\text{BH}_4)_2$, 30 times faster than pristine LiBH_4 (0.45 wt% per h). The findings indicate that the idea of using higher χ_p of metal ions Mg^{2+} to partially substitute the Li cations to form a dual-cation borohydride Li-Mg-B-H truly improves both the dehydrogenation thermodynamics and kinetics of LiBH_4 .

Dehydrogenation reaction mechanism

In order to fully understand the dehydrogenation process, the as-prepared Li-Mg-B-H was heated to different temperatures (295 , 395 , and 495°C) according to the DSC-MS and TPD results and the decomposed products were collected and applied with XRD and FTIR measurements, displayed in Fig. 6. In the XRD



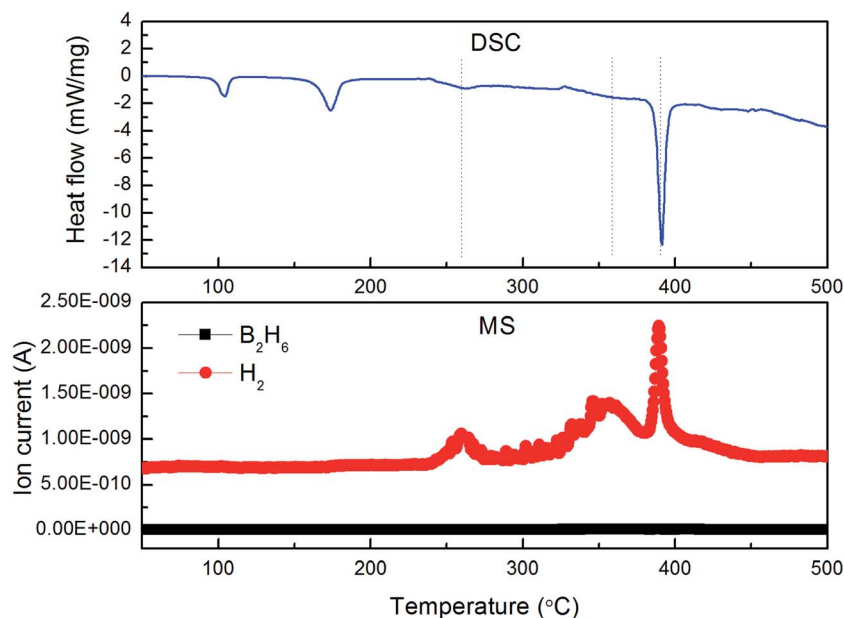


Fig. 4 DSC and MS profiles of Li-Mg-B-H at a heating rate of 5 °C min⁻¹ from room temperature to 500 °C.

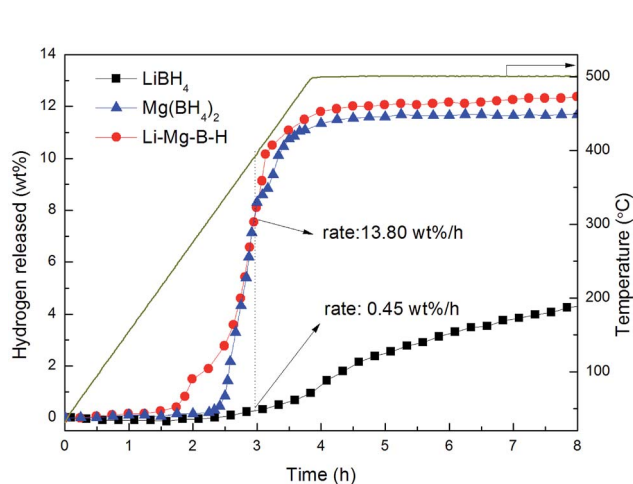


Fig. 5 TPD profiles of LiBH₄, Mg(BH₄)₂ and Li-Mg-B-H at a heating rate of 2 °C min⁻¹ from room temperature to 500 °C under 4 bar initial hydrogen pressure.

patterns, Fig. 6b shows that high-temperature phase of LiBH₄, MgH₂ and MgO (MgO comes from the air contamination of the sample during operation) formed after heated at 295 °C. From the FTIR profile in Fig. 6b, we can see that the peaks of the B-H bonding at 2291, 2223 and 1125 cm⁻¹, which confirm the presence of LiBH₄.⁶ When heated up to 395 °C, metallic Mg and MgO are the only phases detected by XRD, whereas the diffraction peaks of MgH₂ are completely absent. The FTIR pattern shows that LiBH₄ still exists. So in this step, MgH₂ decomposes to Mg and H₂. As the dehydrogenation temperature further increases to 495 °C, the final products are Mg, MgO, MgB₂ and LiH. And the peaks of B-H bonds disappear in FTIR, indicating the complete decomposition of LiBH₄. To sum up, the main decomposition pathway of the new compound under four bar initial hydrogen pressure can be described as follows:

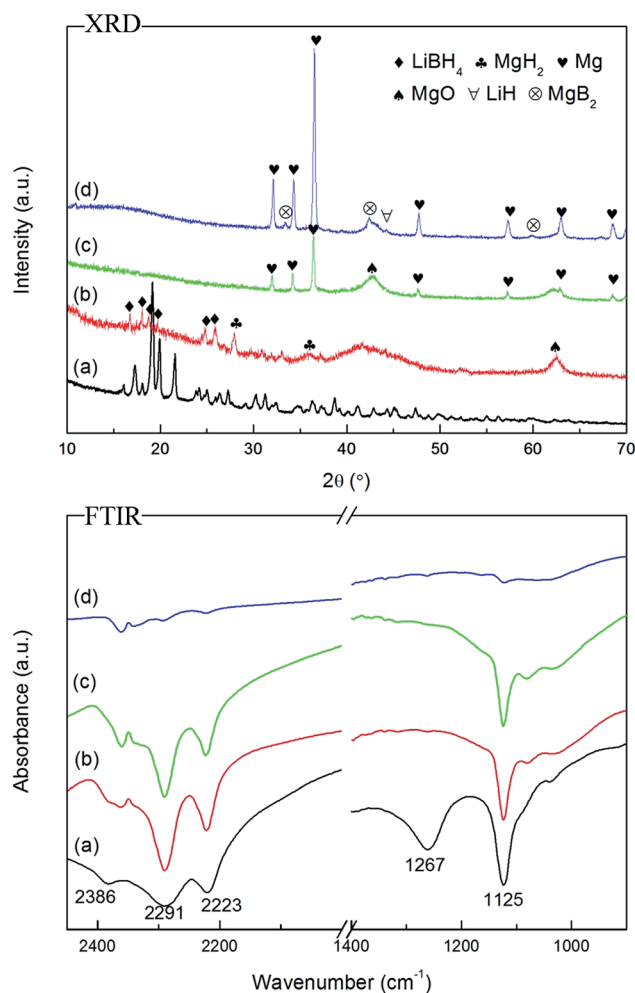


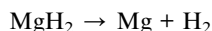
Fig. 6 XRD patterns and FTIR spectra of Li-Mg-B-H decomposed at different temperatures: (a) room temperature, (b) 295 °C, (c) 395 °C, and (d) 495 °C.



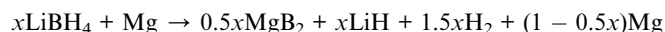
(Step 1)



(Step 2)



(Step 3)



Hydrogen storage reversibility

Reversibility is one of the key features for hydrogen storage materials, especially for on-board applications. In order to study the reversibility of the new compound, we use temperature programmed absorption as well as isothermal rehydrogenation. Fig. 7a shows the temperature absorption curve from room temperature to 500 °C with a heating rate of 2 °C min⁻¹. The pressure is increasing linearly before the temperature is heated to 420 °C, while maintaining and even decreasing when the temperature is above 420 °C. This indicates that the

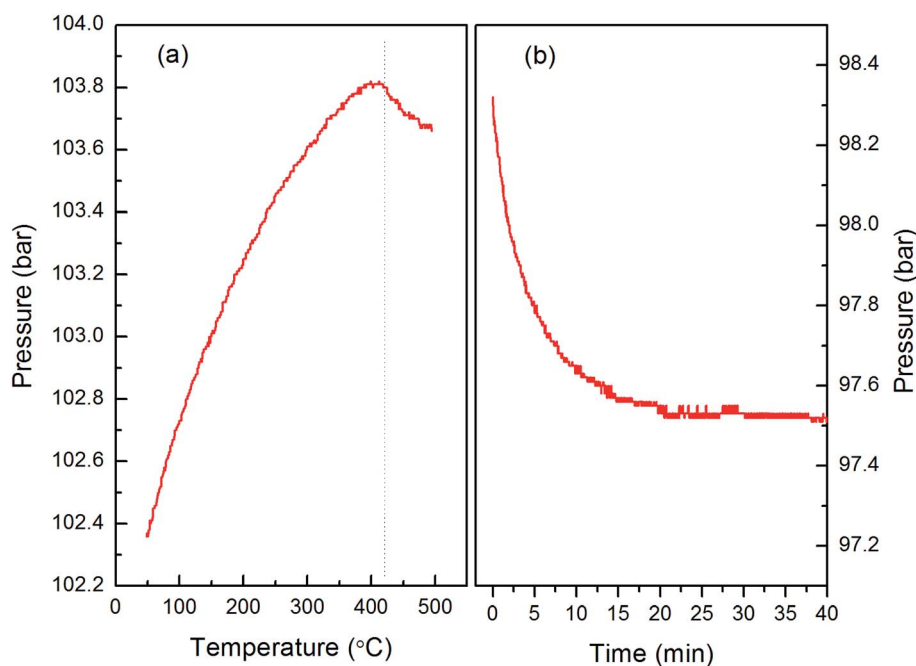


Fig. 7 The rehydrogenation curves of the dehydrogenated sample of Li-Mg-B-H: (a) temperature programmed absorption from room temperature to 500 °C at a heating rate of 2 °C min⁻¹ and (b) isothermal rehydrogenation at 420 °C.

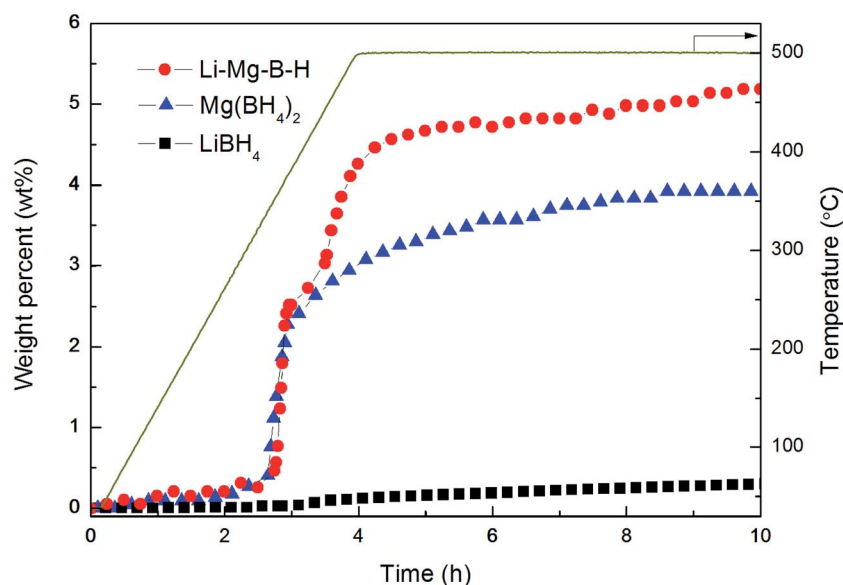


Fig. 8 Hydrogen desorption curve at a heating rate of 2 °C min⁻¹ of the rehydrogenated sample.



dehydrogenated product of Li-Mg-B-H could be rehydrogenated at about 420 °C. From the isothermal rehydrogenation curve at 420 °C in Fig. 7b, the reduction in hydrogen pressure is related to the amount of absorbed hydrogen. XRD patterns (see in Fig. S4†) show that the rehydrogenated sample is composed of MgH₂ and LiBH₄. The dehydrogenation performance of the rehydrogenated sample was further carried out. The dehydrogenation curve is shown in Fig. 8, and it can be observed that the rehydrogenated products can release 5.3 wt% hydrogen, indicating that the new compound has certain reversibility. Nevertheless, this is a great improvement for the reversibility of Li-Mg-B-H comparing with a previous work,³¹ which can only be rehydrogenated to MgH₂ and release about 2 wt% hydrogen. Owing to the complexity of Li-Mg-B-H, detailed experimental and theoretical studies are still required to better understand the cyclic de/rehydrogenation behaviors of the Li-Mg-B-H system.

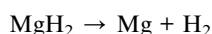
Conclusion

In summary, a new dual-cation borohydride Li-Mg-B-H has been successfully synthesized by ball-milling 3LiBH₄ + MgCl₂ mixture in Et₂O. Further investigations show that dehydrogenation performance of the new Li-Mg-B-H was affected by initial hydrogen pressure. Under four bar initial hydrogen pressure, the onset dehydrogenation temperature of Li-Mg-B-H (250 °C) is 70 °C and 50 °C lower compared to pristine LiBH₄ and Mg(BH₄)₂, respectively. The Li-Mg-B-H can release 12.3 wt% hydrogen from room temperature to 500 °C according to the following three steps:

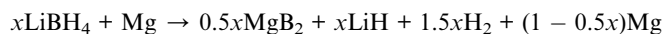
(Step 1)



(Step 2)



(Step 3)



In addition, partial reversibility of Li-Mg-B-H has been demonstrated and 5.3 wt% hydrogen can be released in the second cycle. According to the experimental results of this work, the strategy of altering the χ_p of metal ions in LiBH₄ can truly improve the hydrogen storage properties of LiBH₄ and it may provide general guidance and inspiration in dual-cation borohydrides hydrogen storage materials with advanced and controllable performances.

Acknowledgements

The authors gratefully acknowledge the financial supports for this research from the National Natural Science Foundation of China (51671173, 51571179 and 51471151), the Program for

Innovative Research Team in University of Ministry of Education of China (IRT13037) and the Scientific Research Starting Foundation of Jiangsu University of Science and Technology (1142931607).

References

- 1 M. Felderhoff, C. Weidenthaler, R. von Helmolt and U. Eberle, Hydrogen storage: the remaining scientific and technological challenges, *Phys. Chem. Chem. Phys.*, 2007, **9**, 2643–2653.
- 2 L. Zhang, L. Chen, X. Fan, X. Xiao, J. Zheng and X. Huang, Enhanced hydrogen storage properties of MgH₂ with numerous hydrogen diffusion channels provided by Na₂Ti₃O₇ nanotubes, *J. Mater. Chem. A*, 2017, **5**, 6178–6185.
- 3 L. Schlapbach and A. Züttel, Hydrogen-storage materials for mobile applications, *Nature*, 2001, **414**, 353–358.
- 4 A. Züttel, S. Rentsch, P. Fischer, P. Wenger, P. Sudan, P. h. Mauron and C. h. Emmenegger, Hydrogen storage properties of LiBH₄, *J. Alloys Compd.*, 2003, **356**, 515–520.
- 5 C. Luo, H. Wang, T. Sun and M. Zhu, Enhanced dehydrogenation properties of LiBH₄ compositing with hydrogenated magnesium-rare earth compounds, *Int. J. Hydrogen Energy*, 2012, **37**, 13446–13455.
- 6 Y. Zhao, Y. Liu, H. Liu, H. Kang, K. Cao, Q. Wang, C. Zhang, Y. Wang, H. Yuan and L. Jiao, Improved dehydrogenation performance of LiBH₄ by 3D hierarchical flower-like MoS₂ spheres additives, *J. Power Sources*, 2015, **300**, 358–364.
- 7 H. Liu, L. Jiao, Y. Zhao, K. Cao, Y. Liu, Y. Wang and H. Yuan, Improved dehydrogenation performance of LiBH₄ by confinement into porous TiO₂ micro-tubes, *J. Mater. Chem. A*, 2014, **2**, 9244–9250.
- 8 O. Friedrichs, J. W. Kim, A. Remhof, F. Buchter, A. Borgschulte, D. Wallach, Y. W. Cho, M. Fichtner, K. H. Oh and A. Züttel, The effect of Al on the hydrogen sorption mechanism of LiBH₄, *Phys. Chem. Chem. Phys.*, 2009, **11**, 1515–1520.
- 9 G. Xia, Y. Guo, Z. Wu and X. Yu, Enhanced hydrogen storage performance of LiBH₄-Ni composite, *J. Alloys Compd.*, 2009, **479**, 545–548.
- 10 Y. Guo, X. Yu, L. Gao, G. Xia, Z. Guo and H. Liu, Significantly improved dehydrogenation of LiBH₄ destabilized by TiF₃, *Energy Environ. Sci.*, 2010, **3**, 465–470.
- 11 W. Cai, H. Wang, D. Sun and M. Zhu, Nanosize-controlled reversibility for a destabilizing reaction in the LiBH₄-NaH_{2+x} system, *J. Phys. Chem. C*, 2013, **117**, 9566–9572.
- 12 P. Mauron, M. Biemann, A. Remhof, A. Züttel, J. H. Shim and Y. W. Cho, Stability of the LiBH₄/CeH₂ composite system determined by dynamic PCT measurements, *J. Phys. Chem. C*, 2010, **114**, 16801–16805.
- 13 F. C. Gennari, L. F. Albanesi, J. A. Puszkiel and P. A. Larochette, Reversible hydrogen storage from 6LiBH₄-MCl₃ (M = Ce, Gd) composites by in situ formation of MH₂, *Int. J. Hydrogen Energy*, 2011, **36**, 563–570.
- 14 F. E. Pinkerton and M. S. Meyer, Reversible hydrogen storage in the lithium borohydride-calcium hydride coupled system, *J. Alloys Compd.*, 2008, **464**, L1–L4.



- 15 J. J. Vajo, W. Li and P. Liu, Thermodynamic and kinetic destabilization in $\text{LiBH}_4/\text{Mg}_2\text{NiH}_4$: promise for borohydride based hydrogen storage, *Chem. Commun.*, 2010, **46**, 6687–6689.
- 16 D. Liu, Q. Liu, T. Si, Q. Zhang, F. Fang, D. Sun, L. Ouyang and M. Zhu, Superior hydrogen storage properties of LiBH_4 catalyzed by $\text{Mg}(\text{AlH}_4)_2$, *Chem. Commun.*, 2011, **47**, 5741–5743.
- 17 A. Surrey, C. B. Minella, N. Fechner, M. Antonietti, H. J. Grafe and L. Schultz, Improved hydrogen storage properties of LiBH_4 via nanoconfinement in micro- and mesoporous aerogel-like carbon, *Int. J. Hydrogen Energy*, 2016, **41**, 5540–5548.
- 18 P. Negen, P. Adelhelm, A. M. Beale, K. P. de Jong and P. E. de Jong, $\text{LiBH}_4/\text{SBA-15}$ nanocomposites prepared by melt infiltration under hydrogen pressure: synthesis and hydrogen sorption properties, *J. Phys. Chem. C*, 2010, **114**, 6163–6168.
- 19 P. Javadian, D. A. Sheppard, C. E. Buckley and T. R. Jensen, Hydrogen storage properties of nanoconfined $\text{LiBH}_4\text{--Ca}(\text{BH}_4)_2$, *Nano Energy*, 2015, **11**, 96–103.
- 20 P. Choudhury, S. S. Srinivasan, V. R. Bhethanabotla, Y. Goswami, K. McGrath and E. K. Stefanakos, Nano-Ni doped Li–Mn–B–H system as a new hydrogen storage candidate, *Int. J. Hydrogen Energy*, 2009, **34**, 6325–6334.
- 21 B. Zhai, X. Xiao, W. Lin, X. Huang, X. Fan, S. Li, H. Ge, Q. Wang and L. Chen, Enhanced hydrogen desorption properties of $\text{LiBH}_4\text{--Ca}(\text{BH}_4)_2$ by synergetic effect of nanoconfinement and catalysis, *Int. J. Hydrogen Energy*, 2016, **41**, 17462–17470.
- 22 J. Y. Lee, D. Ravnsbæk, Y. S. Lee, Y. Kim, Y. Cerenius, J. H. Shim, T. R. Jensen, N. H. Hur and Y. W. Cho, Decomposition reactions and reversibility of the $\text{LiBH}_4\text{--Ca}(\text{BH}_4)_2$ composite, *J. Phys. Chem. C*, 2009, **113**, 15080–15086.
- 23 Y. Zhang, Q. Tan, H. Chu, J. Zhang, L. Sun and Z. Wen, Hydrogen de/resorption properties of the $\text{LiBH}_4\text{--MgH}_2\text{--Al}$ system, *J. Phys. Chem. C*, 2009, **113**, 21964–21969.
- 24 P. Ngene, M. van Zwienen and P. E. de Jongh, Reversibility of the hydrogen desorption from LiBH_4 : a synergetic effect of nanoconfinement and Ni addition, *Chem. Commun.*, 2010, **46**, 8201–8203.
- 25 Z. Zhao-Karger, R. Witter, E. G. Bardaji, D. Wang, D. Cossement and M. Fichtner, Altered reaction pathways of eutectic $\text{LiBH}_4\text{--Mg}(\text{BH}_4)_2$ by nanoconfinement, *J. Mater. Chem. A*, 2013, **1**, 3379–3386.
- 26 P. Choudhury, S. S. Srinivasan, V. R. Bhethanabotla, Y. Goswami, K. McGrath and E. K. Stefanakos, Nano-Ni doped Li–Mn–B–H system as a new hydrogen storage candidate, *Int. J. Hydrogen Energy*, 2009, **34**, 6325–6334.
- 27 H. W. Li, S. Orimo, Y. Nakamori, K. Miwa, N. Ohba, S. Towata and A. Züttel, Materials designing of metal borohydrides: Viewpoints from thermodynamical stabilities, *J. Alloys Compd.*, 2007, **446**, 315–318.
- 28 Y. Nakamori, K. Miwa, A. Ninomiya, H. W. Li, N. Ohba, S. Towata, A. Züttel and S. Orimo, Thermodynamical stabilities of metal-borohydrides, *Phys. Rev. B*, 2006, **74**, 045126.
- 29 K. Jiang, X. Xiao, S. Deng, M. Zhang, S. Li, H. Ge and L. Chen, A Novel Li–Ca–B–H Complex Borohydride: Its Synthesis and Hydrogen Storage Properties, *J. Phys. Chem. C*, 2011, **115**, 19986–19993.
- 30 C. Kim, S. Hwang, R. C. Bowman Jr, J. W. Reiter, J. A. Zan, J. G. Kulleck, H. Kabbour, E. H. Majzoub and V. Ozolins, $\text{LiSc}(\text{BH}_4)_4$ as a hydrogen storage material: multinuclear high-Resolution solid-state NMR and first-Principles Density functional Theory Studies, *J. Phys. Chem. C*, 2009, **113**, 9956–9968.
- 31 Z. Fang, X. Kang, P. Wang, H. Li and S. I. Orimo, Unexpected dehydrogenation behavior of $\text{LiBH}_4/\text{Mg}(\text{BH}_4)_2$ mixture associated with the in situ formation of dual-cation borohydride, *J. Alloys Compd.*, 2010, **491**, L1–L4.
- 32 E. G. Bardaji, Z. Zhao-Karger, N. Boucharat, A. Nale, M. J. van Setten, W. Lohstroh, E. Röhm, M. Catti and M. Fichtner, $\text{LiBH}_4\text{--Mg}(\text{BH}_4)_2$: a physical mixture of metal borohydrides as hydrogen storage material, *J. Phys. Chem. C*, 2011, **115**, 6095–6101.
- 33 G. L. Soloveichik, M. Andrus, Y. Gao, J. Zhao and S. Kniajanski, Magnesium borohydride as a hydrogen storage material: synthesis of unsolvated $\text{Mg}(\text{BH}_4)_2$, *Int. J. Hydrogen Energy*, 2009, **34**, 2144–2152.
- 34 K. Chłopek, C. Frommen, A. Léon, O. Zabara and M. Fichtner, Synthesis and properties of magnesium tetrahydroborate, $\text{Mg}(\text{BH}_4)_2$, *J. Mater. Chem.*, 2007, **17**, 3496–3503.
- 35 H. Kou, X. Xiao, L. Chen, S. Li and Q. Wang, Formation mechanism of MgB_2 in $2\text{LiBH}_4 + \text{MgH}_2$ system for reversible hydrogen storage, *Trans. Nonferrous Met. Soc. China*, 2011, **21**, 1040–1046.

